DE83013714

HYDRODYNAMIC STUDY OF A FISCHER-TROPSCH BUBBLE-COLUMN SLURRY REACTOR

MASSACHUSETTS INST. OF TECH., OAK RIDGE, TN. SCHOOL OF CHEMICAL ENGINEERING PRACTICE

JUN 1983

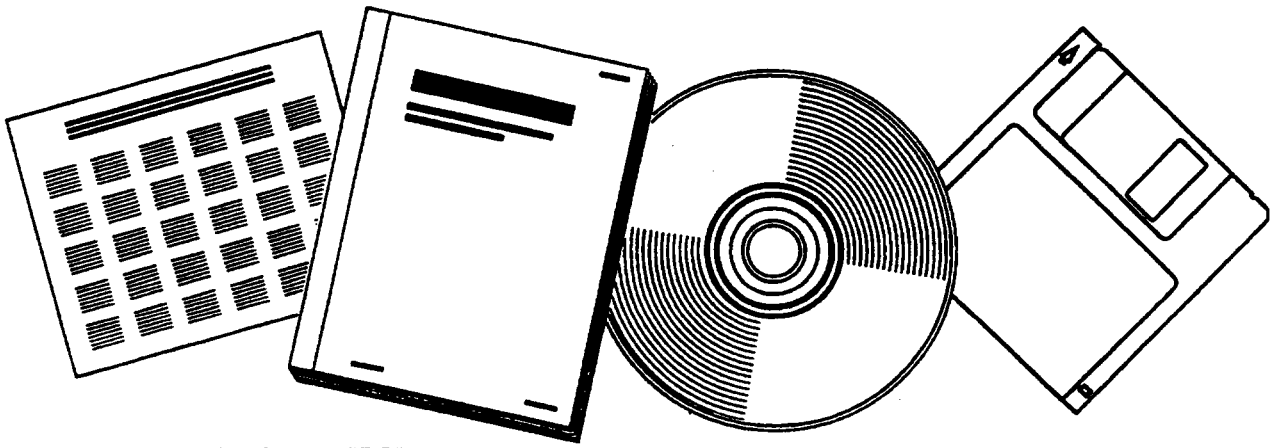

U.S. DEPARTMENT OF COMMERCE
National Technical Information Service

Contract No. W-7405-eng-26

CHEMICAL TECHNOLOGY DIVISION

HYDRODYNAMIC STUDY OF A FISCHER-TROPSCH BUBBLE-COLUMN SLURRY REACTOR

Richard H. Humphreys, Jr.
A. Joseph Antos
Dana P. Woods

Consultants:
R. M. Wham, J. S. Watson, and B. R. Rodgers

Date Published - June 1983

Oak Ridge Station
School of Chemical Engineering Practice
Massachusetts Institute of Technology
G. A. Huff, Jr., Director

Oak Ridge National Laboratory
Oak Ridge, Tennessee 37830
Operated by
Union Carbide Corporation
for the
Department of Energy

ABSTRACT

Hydrodynamic studies were performed to simulate a Fischer-Tropsch reactor in a Plexiglas column 5.08-cm ID and 183-cm tall. Hexane was used in a batch-liquid operation; nitrogen was sparged through a fritted stainless-steel disc. Bubble size was affected by axial position in the column and pore size of the gas sparger. Within experimental error, bubble size was not dependent on gas velocity. Gas holdup was expressed as a function of gas velocity by:

$$\varepsilon_g = 0.0694\ U_g^{0.976}$$

Four generalized correlations for predicting gas holdup were surveyed, but none were found to satisfactorily predict our data. However, data obtained from other Fischer-Tropsch systems were in good agreement with our experimental data. The presence of solids decreased gas holdup up to 50% for superficial gas velocities above 1.5 cm/s. At a gas velocity of 1.5 cm/s, the flow regime changed from bubbly flow to semiturbulent (swirling bubbly).

CONTENTS

1. SUMMARY

Synthetic fuels produced by the Fischer-Tropsch (F-T) synthesis are an attractive alternative to petroleum-based fuels for use as a transportation fuel because the feedstock of the F-T reaction, carbon monoxide and hydrogen, can be derived from coal. The bubble-column slurry reactor (BCSR) is a promising type of reactor for the F-T reaction because it allows better temperature control than other reactor types. The objectives of this project were to investigate hydrodynamic behavior in a mockup column designed to simulate conditions in an F-T bubble-column reactor and to determine hydrogen and carbon monoxide conversion along with product distribution.

By measuring the expanded and stagnant bed height in a Plexiglas mockup, the gas holdup was obtained as a function of superficial gas velocity with and without added solids. For no suspended solids with a 20-μm fritted-glass gas distributor, the expression:

$$\varepsilon_g = 0.0694\ U_g^{0.976} \qquad (1)$$

was empirically fitted to the experimental data. Four generalized correlations were compared with our experimental data on gas holdup in the absence of solids; none showed good agreement. However, the experimental data of Derkwer et al. (9), taken in a Fischer-Tropsch system, agreed closely with our experimental data. In the presence of solids (13 wt % sand particles in the size range of 25-45 μm), our experimental data were compared with three literature correlations that predicted the effects of solids on gas holdup. None of the three correlations was in agreement with our data over the range of gas velocities studied (0 to 3 cm/s). Discrepancies may have occurred because of an observed change in flow regime at a gas velocity of approximately 1.5 cm/s, below which homogeneous bubbly flow was observed, and above which a semiturbulent (swirling bubbly) regime was seen.

Bubble size was measured by stroboscopic photography, and the effects of superficial gas velocity, gas-distributor pore size, and column axial position were investigated. Gas bubbles coalesced as they moved up the column at a superficial gas velocity greater than 1.5 cm/s. Gas-distributor size had a moderate effect, and gas velocity had little effect on bubble size. Average bubble sizes were in agreement with those reported by Dyer et al. (12). The effect of gas-distributor pore size on bubble size conflicted with the findings of Akita and Yoshida (2).

Problems were encountered in starting and operating the bench-scale reactor. The catalyst was reduced at 673 K and a hydrogen flow rate of about 10 STD L/min. Although conversions of 8 to 100% were calculated by using a volume-contraction method, off-gas analysis shows no product

formation. The volume contracted because of a leak in the reactor; when isolated at 1170 kPa, the reactor pressure dropped from 1170 kPa to 790 kPa in 5 min. Also, after less than two days on stream, the reactor was taken off-stream to remove a plug of solidified carrier from the inlet line. Upon restart-up, it is likely that the catalyst was reoxidized and deactivated by air that had diffused into this upstream line. The deactivated catalyst converted no synthesis gas, thus no valid conversion data were obtained from the BCSR.

Further work should include determination of the effects of particle size and density on gas holdup, and the extent of liquid backmixing. A model to predict conversion of the F-T synthesis in the BCSR should be developed.

2. INTRODUCTION

2.1 Background

Interest in alternatives to petroleum-based fuels has increased greatly in recent years. One of the most promising alternatives is the Fischer-Tropsch (F-T) process, in which carbon monoxide and hydrogen from coal gasification react over a catalyst (such as iron or cobalt) to produce mainly linear hydrocarbon chains suitable for use as diesel fuel (19).

The F-T reaction can be written as:

$$CO + 2H_2 \rightarrow (-CH_2-) + H_2O \qquad \Delta H = -150 \text{ kJ/mol} \tag{2}$$

Water is then consumed in the water-gas shift reaction, which often proceeds to equilibrium over an iron catalyst:

$$H_2O + CO \rightleftharpoons CO_2 + H_2 \qquad \Delta H = -40 \text{ kJ/mol} \tag{3}$$

At typical F-T reaction conditions on iron (790 to 2370 kPa and 498 to 598 K), the shift reaction is strongly favored. Another reaction that can occur on F-T catalysts is the Boudouard reaction:

$$2CO \rightarrow CO_2 + C \qquad \Delta H = -170 \text{ kJ/mol} \tag{4}$$

in which carbon is deposited.

Fixed- and entrained-bed reactors have been extensively studied for F-T synthesis. Both are used commercially in South Africa by SASOL. However, the bubble column slurry reactor (BCSR) shown in Fig. 1 is becoming increasingly popular. The advantages of this type of reactor over both the fixed- and fluidized-bed reactors are (19):

1. The capability for processing gas of a low hydrogen-to-carbon monoxide ratio. This is advantageous because synthesis gas from coal-gasification processes typically has a low H_2/CO ratio from 0.5 to 1.0. Fixed- and fluidized-bed reactors require hydrogen upgrading to avoid carbon deposition.

2. High conversion can be achieved in a single pass.

3. Formation of nonvolatile waxy hydrocarbons does not impair BCSR performance, whereas the production of waxy hydrocarbons causes catalyst agglomeration in a fluidized-bed reactor and pore-filling in a fixed-bed reactor.

4. The catalyst in a BCSR does not require a high mechanical strength. Catalysts in a fixed-bed reactor require high crush strength, and those in a fluidized-bed require high resistance to attrition.

5. A spatially uniform temperature profile can be achieved in the BCSR because the liquid carrier provides excellent heat transfer. This prevents the "hot spots" which accelerate carbon deposition in fixed-bed reactors.

A drawback of the BCSR is that performance characterization is difficult. This is because of the complex hydrodynamics of the three phases (gas bubble, liquid carrier, and solid catalyst) as well as gas-liquid mass-transfer effects (9, 11).

2.2 Theory

The two major resistances to reaction in a Fischer-Tropsch (F-T) bubble-column slurry reactor (BCSR) are mass transfer and intrinsic reaction (11). Mass-transfer resistance includes gas-liquid, liquid-solid, and pore-diffusion, but because of large liquid-solid interfacial area resulting from the small catalyst size, the major mass-transfer resistance is that at the gas-liquid interface in the liquid phase ("liquid-side controlling").

The rate of mass transfer is determined by $k_L a$, where k_L is the liquid-phase mass-transfer coefficient, and a is the gas liquid interfacial area. Values of k_L have been reported (11); however, the interfacial area is not well known. Gas-liquid interfacial area is determined from the volume occupied by the gas (gas holdup) and gas bubble size.

An important aspect of modeling conversion is a physical model for the reactor, e.g., plug-flow or well-mixed. For a bubble-column

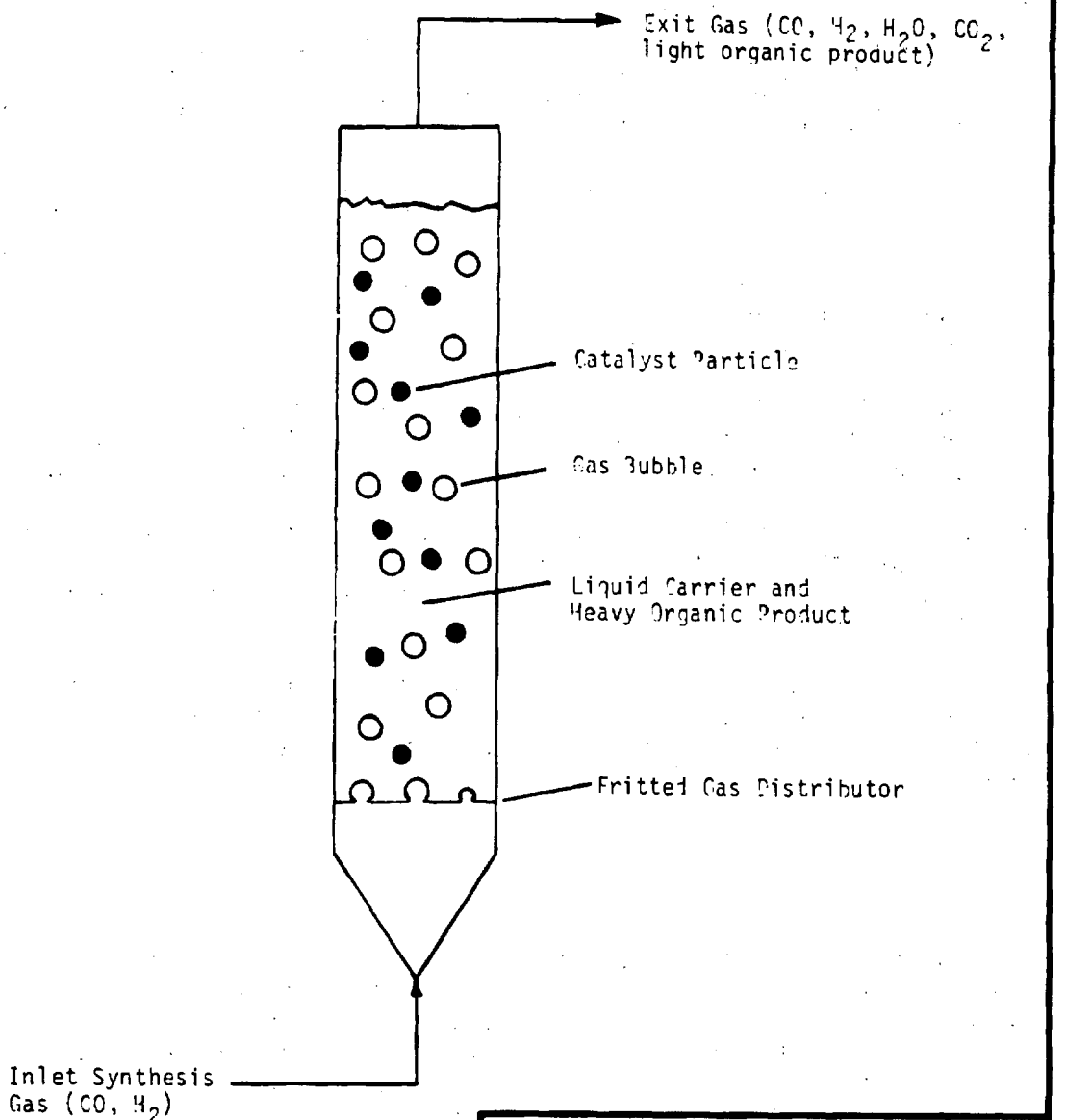

MASSACHUSETTS INSTITUTE OF TECHNOLOGY
SCHOOL OF CHEMICAL ENGINEERING PRACTICE
AT
OAK RIDGE NATIONAL LABORATORY

FISCHER-TROPSCH BUBBLE-COLUMN SLURRY REACTOR

DATE	DRAWN BY	FILE NO.	FIG.
3-23-82	BET	CEPS-X-362	1

reactor, the appropriate physical model depends on the hydrodynamics of the system.

2.3 Objectives and Method of Approach

The objectives of this project were first to experimentally determine gas holdup, bubble size, and flow regime for the operating conditions in a F-T bubble-column slurry reactor (BCSR). With knowledge of these hydrodynamic properties, gas-liquid interfacial area was calculated and an appropriate physical model recommended. The second objective was to measure conversion of hydrogen and carbon monoxide as a function of temperature and space velocity in a F-T slurry reactor.

The approach was divided into two parts:

1. A Plexiglas mockup of the reactor was used to measure bubble size and gas holdup. The liquid carrier employed in the mockup (hexane) at room temperature (293 K) was chosen to simulate the physical properties of a common Fischer-Tropsch BCSR liquid carrier (n-octacosane, $C_{28}H_{58}$) at reaction temperature (518 K). Sand was used to simulate the catalyst particles in studies performed to examine the effects of solids on gas holdup because the density and particle-size distribution were similar to the reduced catalyst.

2. A Fischer-Tropsch BCSR was operated at four temperatures between 513 K and 543 K and four flow rates between 0.5 and 3 L/min. Regrettably, no useful data were generated from this study because of deactivation of the fused-iron catalyst.

3. PREVIOUS WORK

3.1 Gas Holdup

The dependence of the gas holdup on gas velocity is generally of the form (20):

$$\varepsilon_g \propto U_g^{\,n} \tag{5}$$

where

ε_g = gas holdup

U_g = superficial gas velocity

The value of n depends on the flow region. Homogeneous bubbly flow is characterized by uniform bubble density and size, with no coalescence of gas bubbles. The value of n in this regime of flow varies from 0.7 to 1.2. Churn-turbulent flow is characterized by extensive coalescence of bubbles, erratic gas flow, and a high degree of mixing in the gas phase. In the churn-turbulent regime, ε_g is a weaker function of U_g, and n varies from 0.4 to 0.7 (20).

Akita and Yoshida (3) measured gas holdup in a 15.2-cm-ID column. The gas sparge was a single-hole of 5.0-mm diameter. Air, O_2, He, or CO_2 was bubbled into water, methanol, or glycol-water solutions. They proposed that:

$$\frac{\varepsilon_g}{(1 - \varepsilon_g)^4} = 0.2 \left(\frac{g\, D_C^2\, \rho_L}{\sigma}\right)^{1/8} \left(\frac{g\, D_C^3}{\nu_L^2}\right)^{1/12} \left(\frac{U_g}{\sqrt{g\, D_C}}\right) \qquad (6)$$

for physical properties ranging from:

$$800 \text{ kg/m}^3 < \rho_L < 1600 \text{ kg/m}^3$$

$$0.00058 \text{ P} < \mu_L < 0.021 \text{ P}$$

$$0.022 \text{ N/m} < \sigma < 0.0742 \text{ N/m}$$

$$D_C > 15 \text{ cm}$$

where

g = gravitational acceleration
D_C = column diameter
ρ_L = liqiud density
σ = surface tension
ν_L = kinematic viscosity

Hikita et al. (14) investigated the use of gases (air, H_2, CO_2, CH_4, C_3H_8, N_2) in both water and organic liquids. They determined that:

$$\varepsilon_G = 0.672 \left(\frac{U_G \mu_L}{\sigma}\right)^{0.578} \left(\frac{\mu_L^4 g}{\rho_L \sigma^3}\right)^{-0.131} \left(\frac{\varepsilon_G}{\rho_L}\right)^{0.062} \left(\frac{\mu_G}{\mu_L}\right)^{0.107} \quad (7)$$

where

μ_L = liquid viscosity
ρ_G = gas density
μ_G = gas viscosity

The range of applicability of Eq. (7) is the same as that of Eq. (6). In addition, the gas should have a density between 0.84 and 1.84 kg/m^3. This correlation was developed for a 10-cm-diameter bubble column.

The correlation developed by Bach and Pilhofer (4) is valid only for pure organic liquids:

$$\frac{\varepsilon_G}{(1 - \varepsilon_G)} = 0.115 \left[\frac{U_G^3}{\nu_L g(\rho_L - \rho_G)/\rho_L}\right]^{0.23} \quad (8)$$

Equation (7) was developed for gas velocities less than 10 cm/s and column diameters greater than 10 cm.

Hughmark (16) performed studies with air and a variety of liquids. The resulting correlation was:

$$\varepsilon_g = \frac{1}{2 + (0.35/U_G)(\rho_L \sigma/72)^{1/3}} \quad (9)$$

This expression is applicable for the same range of physical properties associated with Eq. (6) and was developed for column diameters greater than 10 cm.

Two studies have been reported for systems specific to F-T synthesis. Calderbank et al. (6) measured gas holdup in both a 5.1-and 25.4-cm-ID bubble column in which nitrogen was sparged through a cone-and-ball sparger into molten wax at 538 K. Their data show a nearly linear dependance of gas holdup on superficial gas velocity for velocities less than 3 cm/s.

Deckwer et al. (9) studied gas holdup in two bubble columns having diameters of 4.1 and 10 cm. The liquid carrier was molten paraffin, and measurements were made at column temperatures of 453 to 513 K with nitrogen. The gas sparger was a sintered-metal plate of a 75-μ mean pore diameter. For this system, Deckwer et al. found that the holdup was nearly a linear function of superficial gas velocity. In comparing their data with that predicted by Eqs. (5) and (7), Deckwer found that the Akita-Yoshida correlation (3) was inaccurate and that the Bach-Philhofer (4) correlation was accurate only at gas velocities less than 1 cm/s. Because one of the columns used in the Deckwer study had a 10-cm diameter and the liquid properties were not in the recommended range, Deckwer et al. concluded that the common holdup correlations are unable to predict the behavior of systems in which Fischer-Tropsch liquid carrier is used.

3.2 Gas Holdup in the Presence of Solids

Begovich and Watson (5) combined the data from six studies for three-phase fluidized beds and proposed the empirical correlation:

$$\varepsilon_g = 1.612\ U_G^{0.720}\ d_p^{0.168}\ D_C^{-0.125} \qquad (10)$$

where

d_p = particle diameter

Most of the data points were from their own study in which air, water, various solids ($\rho_S \approx 2$ g/cm^3), and column diameters of 7.62 and 15.2 cm were used.

Deckwer et al. (9) performed a study in which powdered Al_2O_3 ($d_p < 5$ μm) was introduced in concentrations up to 15 wt % to columns of diameters 4.1 and 10 cm that contained molten wax. The following equation was derived for the slurry column with no liquid flow:

$$\varepsilon_g = 0.0053\ U_G^{1.1} \qquad (11)$$

This correlation was independent of pressure.

3.3 Bubble Size

Akita and Yoshida (2) developed a correlation for bubble size by photographically measuring bubbles. Various liquids and gas distributors were used. On the basis of their data, they proposed the following correlation:

$$\frac{d_{eff}}{D_C} = 26 \left(\frac{D_C^2 \, g \, \rho_L}{\sigma} \right)^{-0.5} \left(\frac{g \, D_C^2}{\nu_L^2} \right)^{-0.12} \left(\frac{U_G}{\sqrt{g \, D_C}} \right)^{-0.12} \tag{12}$$

where

d_{eff} = effective bubble diameter

This relation was developed for columns less than 30 cm in diameter and gas flow rates less than 7 cm/s. These investigators further reported that beyond 30 cm, column diameter does not influence bubble size, and that for a single-orifice sparger, bubble size is independent of orifice size.

Deckwer et al. (8) also observed that orifice size did not strongly influence bubble size. In addition, for their molten-wax system, Deckwer et al. believe that bubble size is independent of gas velocity up to a gas velocity of 3 cm/s (8).

Dyer et al. (12), used isoparaffin to simulate the F-T liquid carrier. They reported that bubble diameter decreased with increasing velocity above 5 cm/s, but below a velocity of about 5 cm/s, bubble sized remained roughly constant.

3.4 Interfacial Area

On the basis of their gas-holdup and bubble-size data, Akita and Yoshida (2) proposed the following correlation for interfacial area:

$$a = \frac{1}{3 \, D_C} \left(\frac{g \, D_C^2 \, \rho_L}{\sigma} \right)^{0.5} \left(\frac{g \, D_C^3}{\nu_L} \right) \varepsilon_g^{1.13} \tag{13}$$

This correlation was developed for the same conditions as their bubble-size and gas-holdup correlations [Eqs. (6) and (12)]. Deckwer et al. (9), using bubble-size and gas-holdup data, reported that:

$$a = 4.5\, U_g^{1.1} \tag{14}$$

This was developed for the same conditions as Eq. (11).

4. EXPERIMENTAL PROCEDURE AND APPARATUS

4.1 Cold-Flow Unit

A Plexiglas mockup column was used to simulate the hydrodynamics of a Fischer-Tropsch bubble-column slurry reactor. The gas holdup (gas volume fraction) with and without suspended solids, the bubble size, and geometry as a function of gas velocity and column position, and the regime of bubbling flow were examined. The influence of gas-distributor pore size on holdup and bubble size was also investigated for two pore sizes.

The mockup column was constructed of 6.35-mm-thick Plexiglas, measuring 5.08 cm in ID and 160 cm in height. Gas was sparged into the bottom of the column through a porous (20 or 100 μm) sintered-metal disc which fit inside a machined section at the lower end of the column. After several runs, the seals between the gas distributor and column loosened, allowing the gas to flow around the gas distributor. General Electric RTV Silicone was then used to seal the outer edge of the gas distributor. Nitrogen was fed to the column with flow regulated by a needle-valve and metered with a wet-test meter. Normal hexane, a liquid which at 293 K simulated the reactor carrier liquid (n-octacosane) at 518 K, was selected for use in the mockup by matching the viscosity, density, and surface tension of the two liquids. The physical properties of n-octacosane at 518 K were estimated by extrapolating viscosity and density from C_{20} and shorter straight-chain paraffins, and surface tension from C_{26} and shorter paraffins (13). The properties of the reactor carrier liquid and the mockup liquid are compared in Table 1.

The mockup was open to the atmosphere, and in all experiments less than 1% evaporation was observed. Surface grazing of the mockup unit occurred because of Plexiglas swelling caused by the hexane, rendering the bottom 10 to 15 cm partially opaque after three weeks. The first set of experiments was performed by varying the superficial velocity of nitrogen between 0.4 to 3.5 cm/s and measuring the stagnant-liquid height and expanded-bed height. Gas holdup ε_g was calculated by:

Table 1. Estimated properties of n-octacosane (518 K) and n-hexane (293 K)

n-octacosane (C_{28})		n-hexane (7)
Density (g/cm^3)	0.80	0.66
Viscosity (cp)	0.57	0.31
Surface tension (dynes/cm)	14.6	18.0

$$\varepsilon_g = \frac{H_{exp} - H_o}{H_{exp}} \tag{15}$$

where

H_{exp} = expanded-bed height
H_o = stagnant-liquid height

Nitrogen was fed to the column for 5 min before starting the experiment to saturate the n-hexane. The flow pattern of the rising gas bubbles was observed in order to characterize flow regimes of homogeneous, turbulent, or slugging two-phase flow. Bubbles were photographed in the mockup using a Polaroid SX-70 camera with a strobe light flashing at 550 flashes/min to investigate the effect of gas velocity on bubble size. A ruler taped to the mockup column was used to gauge the bubble dimensions. Photographs were taken at three superficial gas velocities (0.47, 1.4, and 3.1 cm/s) at a position about midway up the column (35 cm from the bottom in an 80-cm expanded bed). At an intermediate superficial velocity of 1.8 cm/s, bubble photographs were taken at three positions (26, 75, and 110 cm) from the bottom of an expanded bed measuring 135 cm to determine whether bubbles were coalescing as they rose up the column.

In an experiment to examine catalyst settling, fused-iron oxide was added in the mockup column filled with n-hexane. A concentration of 13 wt % iron oxide catalyst (density 5.2 g/cm^3) ground to particle sizes ranging from 37 to 45 and 25 to 37 μm was used. In a similar experiment, sand (density 1.94 g/cm^3) in the same weight concentration and size distribution was used to more closely represent the reduced fused-iron catalyst in the reactor. The effect of catalyst solids on gas holdup was investigated by measuring the stagnant-liquid and expanded-bed heights at gas flow rates of 0.4 to 3.5 cm/s. Equation (15) was used to calculate gas holdup. Bubble-rise velocity was measured in the mockup

column by timing the ascent of gas bubbles up the column. This experiment was performed with a 20-μm frit.

Sedimentation experiments with iron oxide in the mockup demonstrated catalyst-settling problems that warranted further investigation. Upon completion of the reaction studies, the slurry containing fused-iron catalyst at 11 wt % 25-to-45-μm particles suspended in n-octacosane was sampled in the bench-scale BCSR 21.6 and 50.8 cm above the gas distributor for three superficial gas velocities (0.493, 0.946, and 1.3 cm/s). The samples were centrifuged at 3500 rpm for 5 to 10 min in volumetric tubes, and the volume of catalyst and total slurry recorded.

4.2 Bubble-Column Slurry Reactor (BCSR)

4.2.1 Apparatus and Procedure

The BCSR shown in Fig. 2, consisted of a 3.7-L tubular reactor run in a semi-batch operation. Catalyst was suspended in a liquid carrier, through which a mixture of H_2 and CO was bubbled. Hydrogen and CO entered the bottom of the reactor through a 20-μm fritted stainless-steel gas distributor, and volatile products were taken off at the top.

The BCSR was 5.1 cm in diameter and 183 cm high. Four heating rods with temperature controllers were attached to the reactor, and by monitoring center-line temperature with thermocouples, the controllers were set so that the reactor was run isothermally. A 15-μm filter was located at the top of the reactor to prevent catalyst carry over. A back-pressure regulator located downstream of the reactor was used to maintain reactor pressure at 790 kPa. Two traps were used to collect all condensable hydrocarbons: a hot trap at 343 K to condense high-boiling hydrocarbons; and a cold trap at 277 K to collect all other condensables. The flow rate of noncondensable gases was measured with a wet-test meter, as were flow rates of synthesis gas into the reactor.

The catalyst was fused iron (United Catalyst, C-73) crushed to particle sizes of 25 to 37 μm (56%) and 37 to 45 μm (44%). On an unreduced basis the catalyst contained 2.0 to 3.0% Al_2O_3, 0.5 to 0.8% K_2O, 0.7 to 1.2% CaO, and <0.4% SiO_2 (15). Two hundred and ten grams of iron catalyst were introduced to the reactor and reduced with pure H_2 at 698 K for 48 h. The reduction was done at atmospheric pressure and at a H_2 flow rate of 10 L/min. The reduced catalyst was slurried with 1400 g of n-octacosane (99% pure, melting point of 338 K) to produce a suspension of 11-wt-% catalyst on an unreduced basis.

The BCSR was run at four flow rates between 0.5 and 3 L/min, and four temperatures between 513 and 543 K. Flow rates of H_2 and CO into

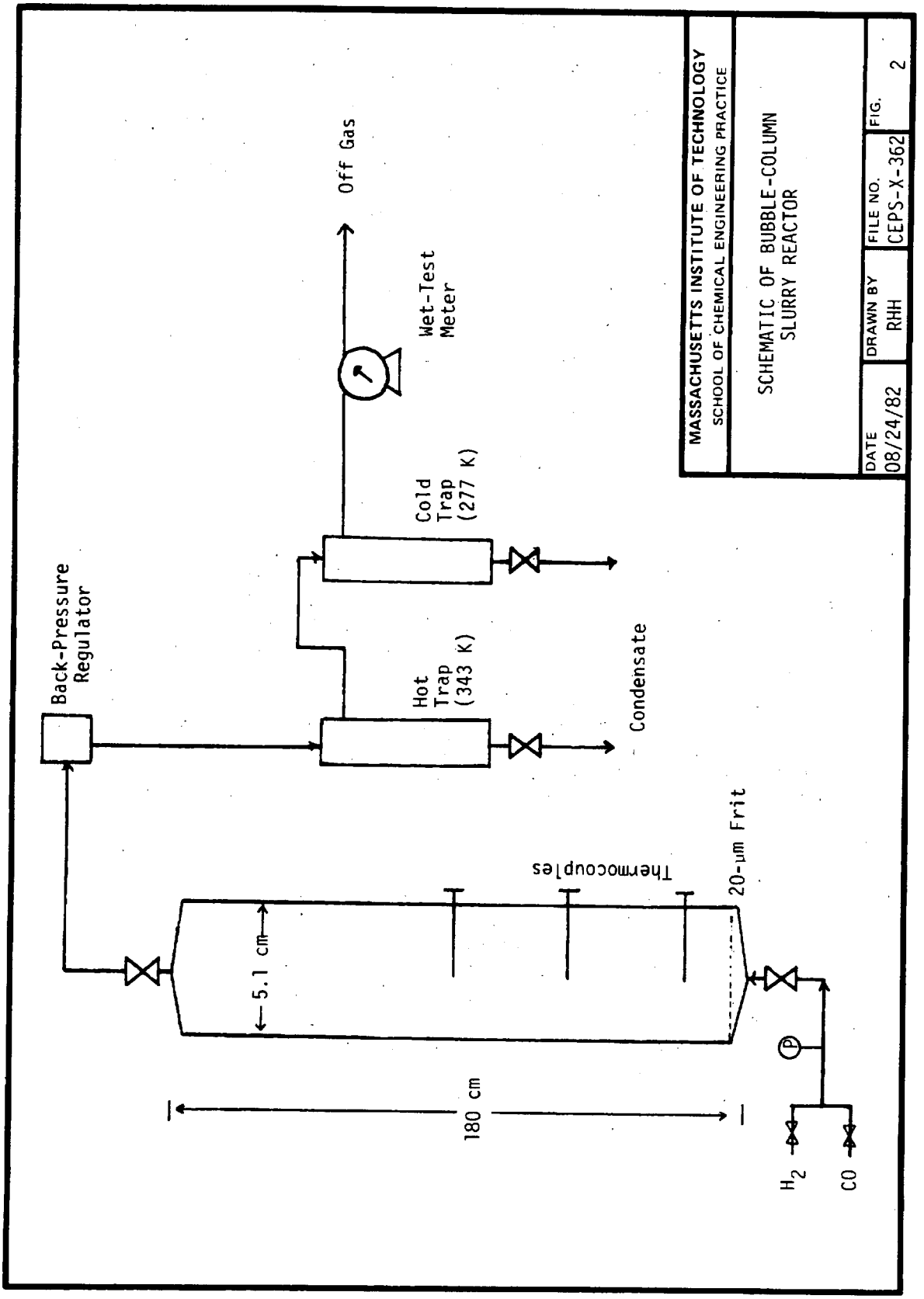
Off Gas
Wet-Test Meter
Cold Trap (277 K)
Hot Trap (343 K)
Condensate
Back-Pressure Regulator
Thermocouples
20-μm Frit
5.1 cm
180 cm
H_2
CO
MASSACHUSETTS INSTITUTE OF TECHNOLOGY
SCHOOL OF CHEMICAL ENGINEERING PRACTICE
SCHEMATIC OF BUBBLE-COLUMN SLURRY REACTOR
DATE 08/24/82
DRAWN BY RHH
FILE NO. CEPS-X-362
FIG. 2

the reactor were controlled by needle valves and measured by bypassing the feed gas to the wet-test meter. The volumetric ratio of H_2 to CO was set at approximately 0.8. The reaction was allowed to reach steady state at each new set of conditions, which was determined by a constant gas flow rate out of the reactor. This usually took 1 to 1.5 h. The outlet flow rate of noncondensable gas was recorded. A gas sample was collected in a glass or stainless-steel bomb and submitted for analysis by gas chromatagraphy. Liquid samples for analysis were collected from either the hot or the cold trap.

4.2.2 Experimental Problems

The BCSR was on-line for approximately three weeks. During this time, conversion measurements were taken by measuring the gas-volume contraction. If a general reaction:

$$6\ CO + 7/2\ H_2 \rightarrow C_3H_7 + 3\ CO_2 \qquad (16)$$

is assumed, then a maximum volume contraction can be calculated (15). Conversion of synthesis gas by this method ranged from 6 to 100% and increased with decreasing flow rate. During this time, no liquid product was collected in either trap. Since there was considerable dead volume (long transfer lines leading from the reactor to the product traps and gas-liquid separators), it was assumed that any liquid product condensed before reaching the traps. Off-gas samples analyzed at M.I.T. by gas chromatography and at ORNL by mass spectroscopy were shown to consist of only CO and H_2 with no CO_2 or hydrocarbons. In other words, no conversion of synthesis gas occurred in the reactor. Deactivation of the catalyst by oxidation was likely responsible for this lack of conversion. After the experiment, the pressure in the isolated reactor decreased from 1100 to 790 kPa in 5 min. A variable leakage of H_2 and CO out of the reactor qualitatively accounts for the volume contraction measured. Gas flow through the leaks would increase at higher superficial gas velocities because of the greater pressure drop through the system. The catalyst may have been reoxidized by accidental exposure to air. Specifically, after less than two days on stream, the reactor was taken off-stream to remove a plug of solidified octacosane (carrier) in the inlet line. Upon restart-up, it is likely that the catalyst was reoxidized and deactivated by air that had diffused into this upstream line. Before the plug developed, an oily substance was collected in the traps, whereas no material was found in the traps after this time.

5. RESULTS

Measured gas holdup is plotted in Fig. 3 as a function of superficial gas velocity. In these experiments, nitrogen was sparged into n-hexane with a 20-μm fritted distributor in the mockup with no solids present. As expected, gas holdup increases steadily with superficial gas velocity; a power-law, least-squares fit of the data produced the relative:

$$\varepsilon_g = 0.0694\ U_G^{0.976} \tag{17}$$

Gas holdup as a function of superficial velocity (no solids present) was also determined for a 100-μm frit and is shown in Fig. 3. Data for these runs are found in Appendix 10.2.

Experiments performed with 13-wt-% sand (density of 1.93 g/cm^3 and particle sizes of 25 to 45 μm) for the 20-μm frit resulted in a markedly different gas holdup as a function of superficial velocity, as shown in Fig. 4. With sand present an apparent transition in flow regime, characterized by increased turbulence and mixing of gas bubbles, occurred between superficial velocities of 1.5 to 1.8 cm/s. However, the finely divided solids made observation difficult. No significant settling of sand particles on the gas distributor was seen over the entire range of superficial velocities (0.4 to 3.4 cm/s). In an experiment with iron oxide particles of the same size distribution (density of 5.2 g/cm^3) at 13 wt %, settling on the distributor was observed over the full range of superficial gas velocities ranging from 0.4 to 3.4 cm/s.

Observation of bubbling and flow conditions in the transparent mockup during gas-holdup experiments showed that bubbly flow occurred at superficial velocities of 0.4 to 1.4 cm/s with no solids present. Above superficial velocities of about 1.8 cm/s, a swirling-bubbly flow occurred, with no turbulence or churning; but bubbles followed a helical trajectory up the column. Transition between these two flow regimes occurred at superficial velocities of 1.4 to 1.8 cm/s.

Photographs of nitrogen bubbles in n-hexane showed that in the gas-velocity range below 2 cm/s, the bubbles were roughly ellipsoidal. Above superficial gas velocity of 2 cm/s, the gas-bubble geometry became increasingly irregular as shown in Fig. 5. Photographs for three superficial velocities at a point 35 cm up the column showed only a slight variation in bubble size, as listed in Table 2. Bubble dimensions were averaged over 15 bubbles. Bubble volumes and areas for ellipsoids are calculated by:

$$\hat{V} = \frac{4\pi}{3}\,(a')^2 b \tag{18}$$

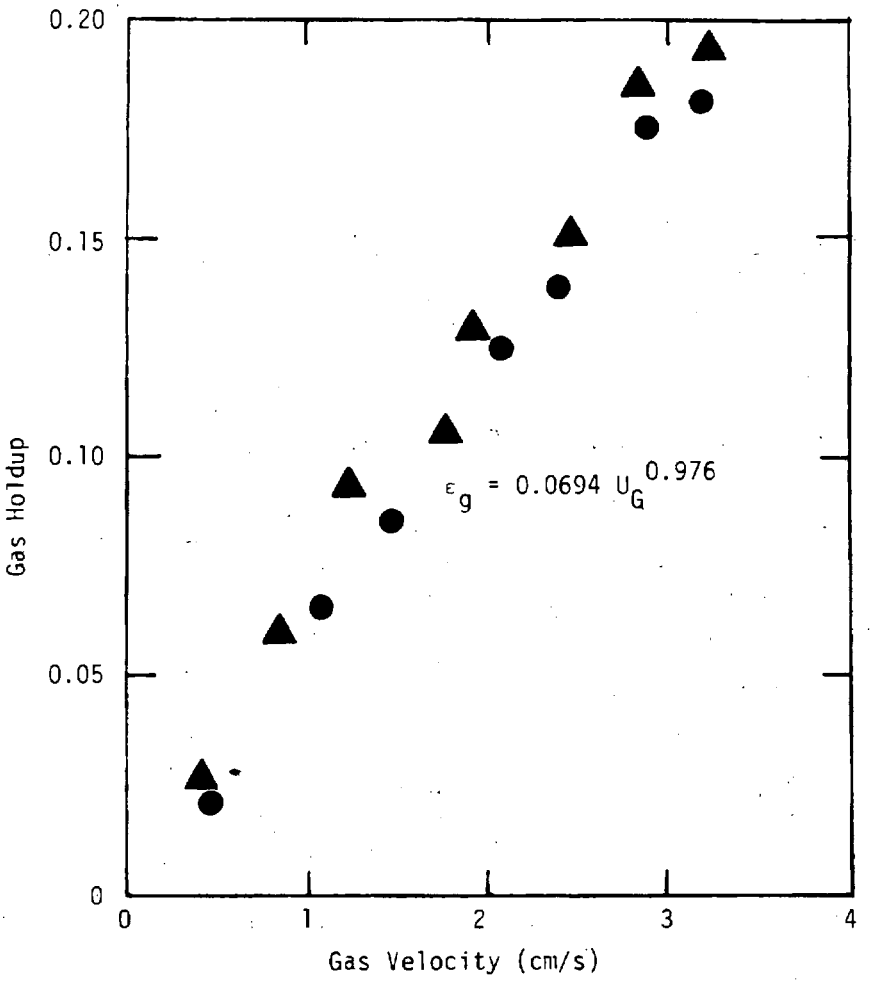

MASSACHUSETTS INSTITUTE OF TECHNOLOGY SCHOOL OF CHEMICAL ENGINEERING PRACTICE AT OAK RIDGE NATIONAL LABORATORY			
GAS HOLDUP WITH 20-μm AND 100-μm FRITTED DISTRIBUTORS			
DATE 09/03/82	DRAWN BY DPW	FILE NO. CEPS-X-362	FIG. 3

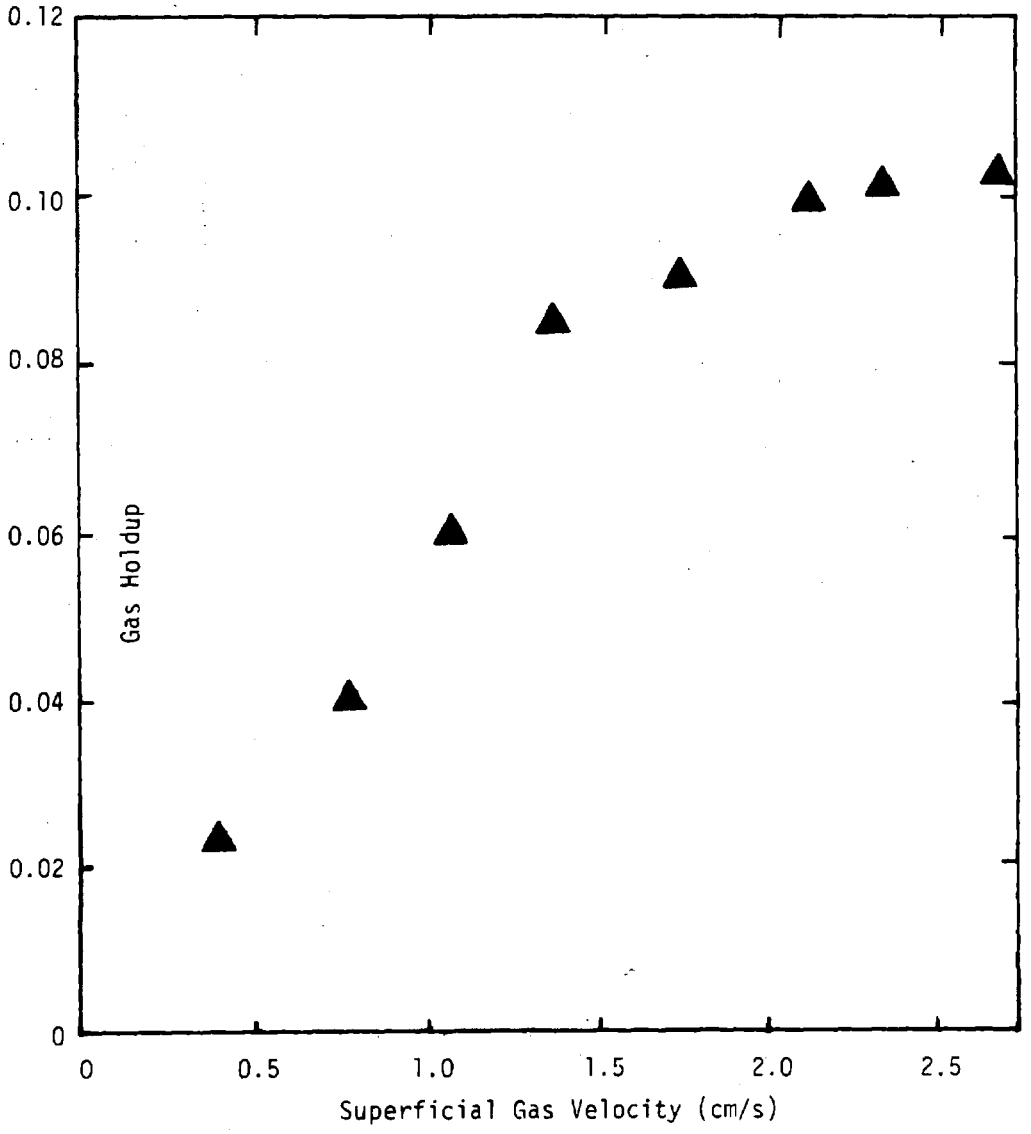

MASSACHUSETTS INSTITUTE OF TECHNOLOGY
SCHOOL OF CHEMICAL ENGINEERING PRACTICE
AT
OAK RIDGE NATIONAL LABORATORY

GAS HOLDUP WITH 13 wt %
25-to-45-μm SAND

DATE	DRAWN BY	FILE NO.	FIG.
08/31/82	DPW	CEPS-X-362	4

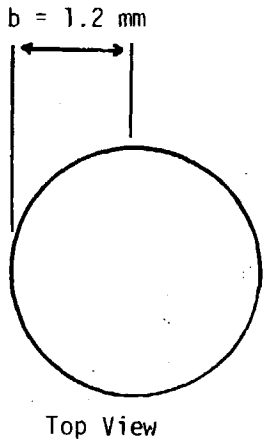

Top View

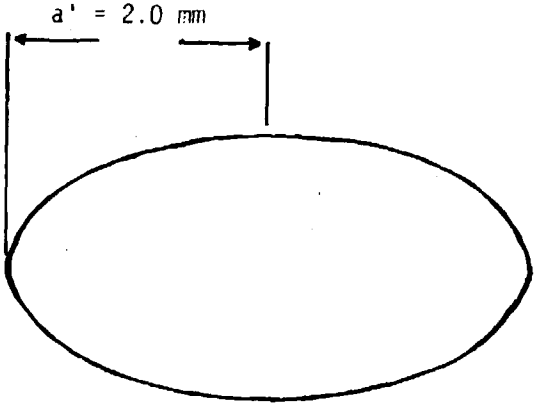

Front View

MASSACHUSETTS INSTITUTE OF TECHNOLOGY SCHOOL OF CHEMICAL ENGINEERING PRACTICE AT OAK RIDGE NATIONAL LABORATORY			
AVERAGE BUBBLE DIMENSIONS 75 cm FROM BOTTOM, 1.77 cm/s			
DATE 08/31/82	DRAWN BY DPW	FILE NO. CEPS-X-362	FIG. 5

Table 2. Variation of bubble size with superficial gas velocity without solids[a]

U_G (cm/s)	Volume equivalent spherical diameter (mm)[b]	Bubble dimensions (mm)		Volume (ml^3)	Area (mm^2)
		Major axis	Minor axis		
0.47	2.85 ± 0.31	3.4 ± 0.3	2.0 ± 0.3	12.1 ± 4.0	21.7 ± 4.1
1.44	2.94 ± 0.20	3.4 ± 0.2	2.2 ± 0.2	13.3 ± 2.8	21.0 ± 3.0
3.04	3.05 ± 0.22	3.5 ± 0.4	2.3 ± 0.3	14.8 ± 5.3	22.4 ± 5.5

[a]Photographs taken at 35 cm above 20-μ frit in an 80-cm expanded bed.
[b]Error is standard deviation of 15 bubble sizes.

where

$\hat{V}$ = bubble volume
a' = major semi-axis
b = minor semi-axis

$$A = 2\pi(a')^2 + \pi \frac{b^3}{3} \ln\left(\frac{1 + \varepsilon}{1 - \varepsilon}\right) \tag{19}$$

where

ε = elipsoid eccentricity
A = bubble area, cm^2

and

$$\varepsilon = \frac{\sqrt{(a')^2 - b^2}}{a'} \tag{20}$$

A sample calculation for bubble diameter is shown in Appendix 10.1. Photographs of bubbles at an intermediate superficial gas velocity of 1.77 cm/s at three column positions showed an increase in bubble size up the column as summarized in Table 3.

Table 3. Variation of bubble size with column position without solids[a]

Height (cm)	Volume equivalent spherical diameter (mm)[b]	Bubble size (mm)		Volume (ml^3)	Area (mm^2)
		Major axis	Minor axis		
26	2.8 ± 0.3	3.6 ± 0.4	1.7 ± 0.2	11.5 ± 3.9	22.1 ± 5.1
75	3.37 ± 0.4	4.0 ± 0.5	2.4 ± 0.2	20.1 ± 6.7	29.1 ± 7.5
110	3.86 ± 0.4	4.9 ± 0.4	2.4 ± 0.3	30.2 ± 9.0	42.6 ± 7.8

[a]All photographs taken at a superficial gas velocity of 1.77 cm/s with 20-μm frit.

[b]Error is standard deviation of 15 bubble sizes.

Bubbles were also photographed 75 cm above the bottom of the column at a superficial velocity of 1.77 cm/s with the 100-μm fritted gas distributor in place. A comparison of this average bubble size with that obtained with the 20-μm frit is shown in Table 4.

Table 4. Effect of gas-distributor pore diameter on bubble size without solids[a]

Distributor pore diameter (μm)	Volume equivalent spherical diameter (mm)[b]	Bubble size (mm)		Volume (ml^3)	Area (mm^2)
		Major axis	Minor axis		
20	3.37 ± 0.4	4.00 ± 0.5	2.4 ± 0.2	20.1 ± 6.8	29.1 ± 7.3
100	3.85 ± 0.5	4.60 ± 0.5	2.7 ± 0.4	29.9 ± 9.0	39.0 ± 9.6

[a]All bubbles photographed at a superficial gas velocity of 1.77 cm/s at a position of 75 cm above the 20-μm frit in a 135-cm expanded-bed.

[b]Error is standard deviation of 15 bubble sizes.